Article

J. Mex. Chem. Soc. **2018**, *62*(2)
Special Issue

ISSN-e 2594-0317
ISSN 1870-249X

Modeling of Hg (II) Adsorption onto Ca-bentonite

Irma Robles[1], Yamir Bandala[2], Juan Manríquez[1] and Erika Bustos[1,*]

[1]Centro de Investigación y Desarrollo Tecnológico en Electroquímica, S. C. Parque Tecnológico Querétaro s/n, Sanfandila, Pedro Escobedo, Querétaro, 76703, Mexico.
[2] Instituto Tecnológico y de Estudios Superiores de Monterrey. Calle del Puente 222, Col. Ejidos de Huipulco, Tlalpan, 14380, México D.F.
***Corresponding author:** Erika Bustos, Ph. D. Phone.: +52 442 2 11 60 59. Fax: +52 442 2 11 60 01. E-mail address: ebustos@cideteq.mx

Received November 19th, 2017; Accepted February 12th, 2018.

DOI: http://dx.doi.org/10.29356/jmcs.v62i2.396

Abstract. The presence of mercury in soils, like other heavy metals, is associated with organic matter and minerals. Mercury deposited in soils is mainly in its oxidized form Hg2+. The adsorption of Hg (II) from aqueous solution into Ca-bentonite was studied. Adsorption percentage was determined as a function of shaking time and temperature to study the thermodynamics and kinetics of Hg (II) adsorption on Ca-bentonite, which was simulated using the MINSQ and GAUSSIAN 09 programs.
Key words: Hg (II); Ca-bentonite; MINSQ; GAUSSIAN 09.

Resumen. La presencia de mercurio en los suelos, al igual que otros metales pesados, está asociada con materia orgánica y minerales. El mercurio depositado en los suelos se encuentra principalmente en su forma oxidada Hg2+. En esta investigación se muestra la adsorción de Hg (II) de una solución acuosa en Ca-bentonita, con el fin de estudiar la termodinámica y la cinética de esta adsorción, la cual fue simulada usando los programas MINSQ y GAUSSIAN 09.
Palabras clave: Hg (II); Ca-bentonita; MINSQ; GAUSSIAN 09.

Introduction

Mercury in soil could be retained, mobilized and volatilized, by different soil processes. They are associated with the presence of organic matter and minerals such as silicate clays, pyrite and quartz; some of which have the capability to adsorb or interchange metal ions. Mercury adsorbed in mineral surfaces depends on pH, cationic interchange capability, and specific surface morphology of soil particles. Mercury is easily sorbed on clay minerals present in soil, for example, clay minerals that are composed of fine particles specifically kaolinites, montmorillonites, and illites. All of these have its own crystal lattice structures and their specific surface areas generally are very high. [1, 2] Among the several clays, montmorillonite, often-called bentonite commercially, has high ion exchange capacity a fine particle size, and specific molecular structure, and for this reason had been used as a clarifying agent in water and wastewater for metal recovery. [3] Different computational tools have been used to model metal adsorption on clay minerals. Quantum, molecular mechanics, and molecular dynamics methods, and also Monte Carlo simulation techniques have been successfully applied to the behavior of clay materials as well as various hydrated cations during adsorption [4-16].

Mercury has a high affinity for soil minerals, so it might expect low mobility of this metal. However, the amount of mercury adsorbed on the mineral surfaces of the soil depends on the soil pH, cation exchange capacity and the specific surface of soil particles [17-19]. Adsorption is the accumulation of a surface active material in two dimensions in a water/solid substrate and is based on intramolecular interactions the adsorbate and the solid phase solute, earlier researchers have shown that clays act as good adsorbent materials. [18, 20-22]

J. Mex. Chem. Soc. **2018**, *62*(2)
Special Issue

ISSN-e 2594-0317
ISSN 1870-249X

Adsorption kinetics depends on the interaction adsorbent-adsorbate and system conditions. The solute adsorption rate determines the residence time required to carry out the adsorption reaction for purification and this process can be analyzed as a chemical kinetic system. [23-25] Mathematical correlation is an important role to the modeling process, where physicochemical parameters are studied with the corresponding thermodynamic considerations. [22] The models corresponding to two parameters can be evaluated directly in a laboratory study of adsorption on an adsorbent material over time. [23, 26-33] Once the amount of mercury adsorbed is known experimentally the model that best fits the adsorption of mercury can be built. [21, 23, 27] The adsorption of Hg (II) on Clay is possible by any of three main mechanisms of interaction, as seen in the equations as 1 to 3 below [21].

Mechanism 1:

$$\text{Ca-bentonite} + Hg^{2+}_{sol} \leftrightarrow \text{Hg–bentonite} + Ca^{2+}_{sol} \quad \text{Eq. 1}$$

Mechanism 2:

$$\text{Ca-bentonite} + 2HgOH^{+}_{sol} \leftrightarrow 2HgOH^{+}\text{–bentonite} + Ca^{2+}_{sol} \quad \text{Eq. 2}$$

Mechanism 3:

$$\text{Ca-bentonite} + 2H^{+}_{sol} \leftrightarrow 2H^{+}\text{–bentonite} + Hg^{2+}_{sol} \quad \text{Eq. 3}$$

Where Ca-bentonite represents the Ca clay, some reports show the formation of different mercury compounds than these mechanisms indicate [18]. Focusing on the last mechanism, adsorption isotherms were developed to analyze the adsorption of mercury on calcium bentonite during this study.

The kinetic and thermodynamic study allowed us to study the behavior of the adsorption of mercury. The observed adsorption kinetic behavior fit a second-order model, when the data were fitted to the Freundlich isotherm, and these results are consistent with the literature pertaining to the adsorption of mercury in various matrices as carbon material by the lateral interactions of mercury over adsorbent material. The results of the thermodynamic study indicate that the adsorption process is favored as $|Hg|_{ads} < |Hg|_{sol}$. This means that an excess of mercury in solution favors the adsorption of mercury in calcium bentonite. Therefore, the energy of the adsorption process is -40.57 $KJ \cdot mol^{-1}$. The mercury is adsorbed onto the calcium bentonite to form a stable bond, where the mercury displaces the calcium in the bentonite, it is present in solution promoting by the kinetic process [34].

This report summarizes the adsorption of Hg (II) from aqueous solution into Ca-bentonite which was studied using a batch technique under controlled temperature and constant pressure. Adsorption percentage was determined as a function of shaking time and temperature to develop the adsorption thermodynamics and kinetics of Hg (II) on Ca-bentonite, which was simulated using the MINSQ and GAUSSIAN 09 programs

Experimental

Calcium and sodium Bentonite from *Lodbent* was used to analyze equilibrium adsorption of mercury, for this purpose Ca-Bentonite was exposed to a solution of mercuric chloride ($HgCl_2$) from Merck. The adsorption process was performed using a Cole Parmer bath temperature control. The system used for this purpose was a 20 mL glass cell, where reagents were placed to study the sorption process under controlled temperature at 25 °C and constant atmospheric pressure. All experiments were performed in duplicate at a neutral pH.

The amount of mercury in solution was determined using Anodic Stripping Voltammetry (ASV), an electrochemical technique used to determine metal concentration in solution, which has a lineal equation $y = 2549.30x - 0.0355$, where y = current density ($\mu A/cm^2$), x = mercury concentration (mol/L), with a $R^2 = 0.993$, detection and quantification limit of 112.043 pM and 0.373 nM, respectively. For this purpose a Basi Epsilon potentiostat and an electrochemical cell with glassy carbon, Pt wire and Ag|AgCl as working electrode (WE), counter electrode (CE) and reference electrode (RE) respectively. In this way the amount of mercury adsorbed on the clay was determined.

After experimental evidence was collected, the Hg^{2+} adsorption behavior was modeled using a computer based (MINSQ and GAUSSIAN 09 Software) [35] model where theoretical and experimental adsorption was compared.

J. Mex. Chem. Soc. **2018**, *62*(2)
Special Issue

ISSN-e 2594-0317
ISSN 1870-249X

Results and Discussion

Adsorption of Hg (II) on Ca-bentonite

The adsorption of Hg^{2+} on Ca and Na-bentonite was followed via ASV, results are shown in Fig. 1 and 2 respectively as the black circles. Additionally, a theoretical model was used to identify bond interactions. This model is based on molecules interactions, where the adsorption process is carried out by adsorption desorption interactions between cations competing by active sites, this model is represented as described by Chen and Frank, is presented in Eq. 4 [36].

$$q_t = \frac{k_a C_0}{k_a C_0 + k_d} q_m \left\{ 1 - \exp\left[-\frac{k_a}{N_0}\left(C_0 + \frac{k_d}{k_a} \right) \right] t \right\} \qquad \text{Eq. 4}$$

where K_a represents the adsorption constant, K_d desorption constant, and C_0 represents initial concentration. q_m represents the equilibrium adsorption capacity of the clay, N_0 the adsorbed concentration by available adsorption sites, and q_t relates total quantity of metal adsorbed by the clay in a time t.

Experimental data of adsorption process represented in Fig. 1 and 2 by the black line (Fig. 1, black circles) where fitted to the model of Chen and Frank. As can be seen in fig. 1 and 2, calcium bentonite has higher sorption capacity, for this purpose this clay was used for modeling and next calculations. Follow this plot thermodynamic parameters k_a, k_d, q_m, N_0 y ΔG^o where calculated, these values are shown in Table 1.

In terms to understand experimental results, further analysis was done using Gaussian 09, results are described below.

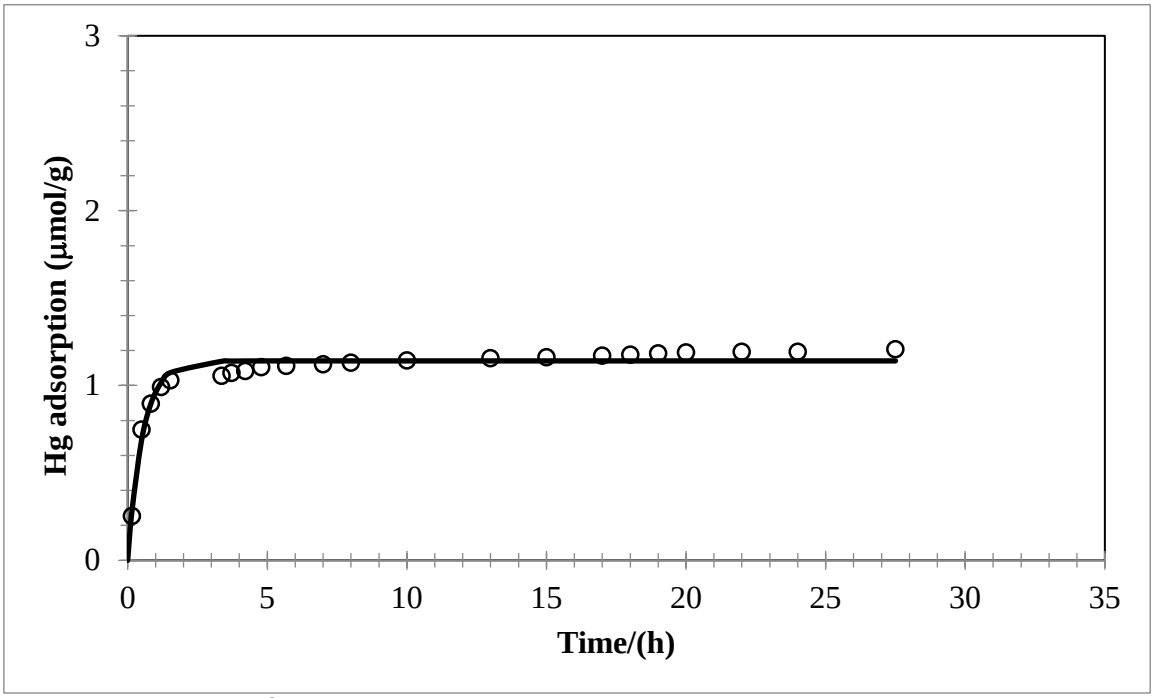

Fig. 1. Adsorption of Hg^{2+} onto Na-bentonite. Carried out at atmospheric pressure, 25°C, and neutral pH.

J. Mex. Chem. Soc. **2018**, *62*(2)
Special Issue

ISSN-e 2594-0317
ISSN 1870-249X

Table 1. Thermodynamic parameters calculated by theoretical model**.**

Parameter	Calcium bentonite
k_a ($L \cdot mmol^{-1}\ h^{-1}$)	1.24 ± 0.12
k_d (h^{-1})	0.08 ± 0.01
q_m (µmol $Hg \cdot g^{-1}$ bentonite)	3.99 ± 0.09
N_0 (µmol $Hg \cdot g^{-1}$ bentonite /µmol sites$\cdot g^{-1}$ bentonite)	0.45 ± 0.05
Θ_{max}	0.675
ΔG^o ($KJ \cdot mol^{-1}$)	-33.58

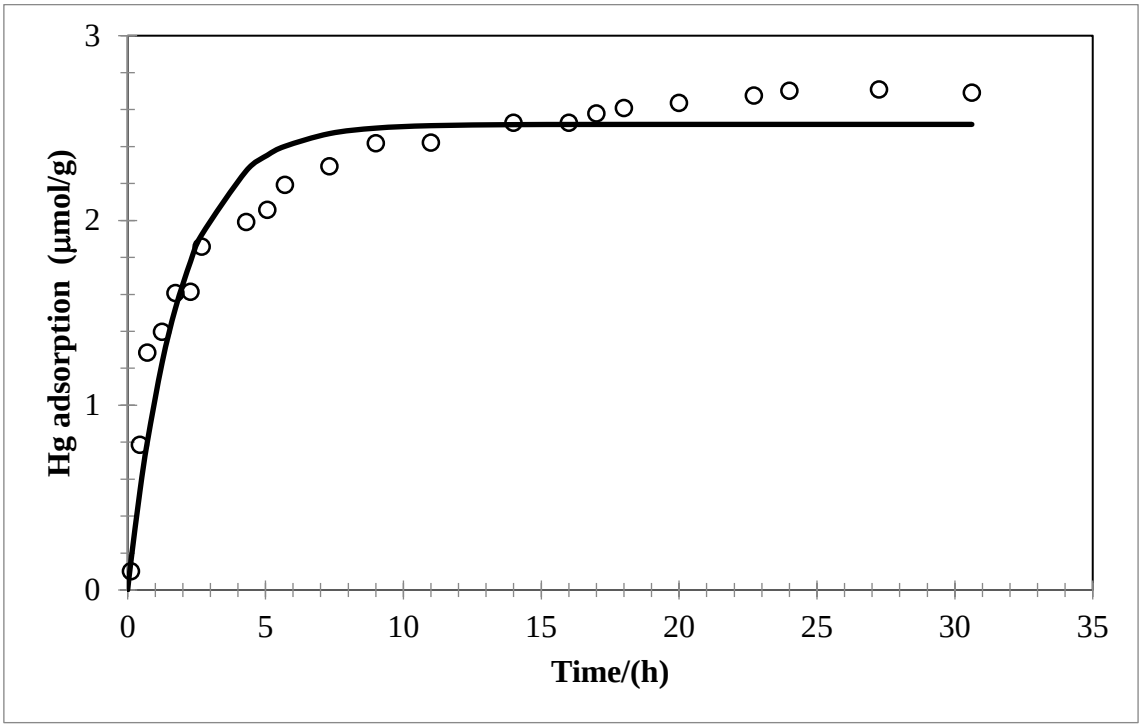

Fig. 2. Adsorption of Hg^{2+} onto Ca-bentonite. Carried out at atmospheric pressure, 25°C, and neutral pH.

Structural and computational models

Bentonite is a complex structure with a highly variant composition, for this reason its principal structure, montmorillonite, was modelled [37]. The isomorphic substitution of montmorillonite prevents the formation of a structure with an explicit localization for the substitutions in the crystallographic data, for this reason the montmorillonite cell model studied was based on the de Mignon *et al., 2010* report [38]. The cell parameters of Ca-montmorillonite described by Viani et al., 2002 [39] (a = 5.18 Å, b = 8.98 Å, c = 15.00 Å, α = 90 Å, 90 Å = β, γ = 90 Å) were taken and duplicate in three directions to form a new cell dimensions a = 11.26676 Å, b = 17.46034 Å, c = 26.8225 Å after adjusting the content of atoms. Calcium atoms were removed, and the hydrated cations of interest were place in their vacated sites.

Montmorillonite has a diffuse negative charge distribution resulting from isomorphous substitution in the octahedral layer. Such distribution may not reflect the replacement of hydrated cations located between the layers [5], so this net negative charge was neutralized by the addition of hydrogen atoms in the montmorillonite crystal model

Hydration of Ca^{2+} and Hg^{2+}

The structure of the hydration sphere of the ions Ca^{2+} and Hg^{2+} is fundamental to understanding their behavior in a given system. Thus, there are many theoretical and experimental reports where probable hydration numbers for Ca^{2+} and Hg^{2+} are described. In the specific case of Ca^{2+}, the more favorable

J. Mex. Chem. Soc. **2018**, *62*(2)
Special Issue

ISSN-e 2594-0317
ISSN 1870-249X

hydration numbers are 6 and 7 that may alloy a second layer which can improve hydration stability. [4, 40-46] A similar situation arises for Hg^{2+} [47-54]. Initially four hydration systems were proposed for Ca^{2+} and Hg^{2+} ions: penta, hexa, hepta and octa-hydrated whose resulting structures were taken as the basis for a second hydration sphere (10 water molecules) for those ions.

Computational results

Quantum mechanical (QM), molecular mechanics (MM), molecular dynamics (MD) methods as well as Monte Carlo (MC) simulation techniques have been successfully applied to the behavior of clay materials as well as various hydrated cations during adsorption. The method of theory density functional (DFT) has proven particularly useful in simulation systems of interest for montmorillonite [5], Ca^{2+} and Hg^{2+} hydrated cations [4,6] and complex cation-montmorillonite. [11, 55-57] The system model for montmorillonite was optimized using molecular mechanics (UFF) [12, 13] using the software Gaussian 09. [35] While optimizing the geometries of the Ca^{2+} and Hg^{2+} hydrated systems using the method of DFT by the functional B3LYP [15] and Lanl2dz [16] base was conducted with the same software. The structures resulting from the optimization process (montmorillonite and hydrated cations) were combined to create the complex hydrated-montmorillonite cation (hydrated cations were located between the layers of montmorillonite). Additionally, it optimized with oniom (B3LYP / LANL2DZ technique: UFF) and implemented in the Gaussian 09 program [58]. All structures resulting from the optimization process were subjected to frequency analysis to ensure that they correspond to a minimum (local) and to estimate the values of enthalpy and free energy of reaction [59].

Geometries

According to the simulation performed for hydration of Ca^{2+} and Hg^{2+}, these cations may form structures with those added water molecules. However, after 6 water molecules, the systems showed a preference for maintaining the coordination number [38]²²²² in its first hydration layer and subsequently forming a second layer with the remaining water molecules (Fig. 3).

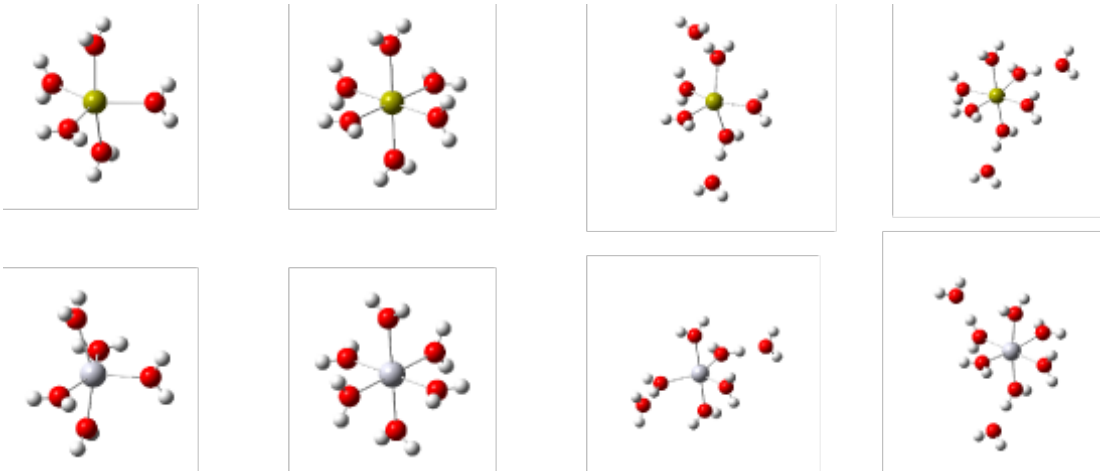

Fig. 3. Coordination Modes for Ca^{2+} and Hg^{2+} ions in the presence of 1 to 8 molecules of water, wherein a preference for a first coordination sphere formed by six water molecules is observed. Upper: Hydration for Ca^{2+}; Lower hydration for Hg^{2+} (B3LYP / LANL2DZ).

In the case of the decahydrated systems for Ca^{2+} and Hg^{2+}, the same trend as previously described occurs, promoting bonding of six water molecules in the first hydration layer and the remainder on a second layer for both cations (Fig. 4).

During the optimization process, the hydrated montmorillonite cation complex, showed that previously described coordination spheres are not changed even though the water molecule hydrated cation are oriented to form hydrogen bonds with the oxygen atoms of the montmorillonite (Fig. 5).

J. Mex. Chem. Soc. **2018**, *62*(2)
Special Issue

ISSN-e 2594-0317
ISSN 1870-249X

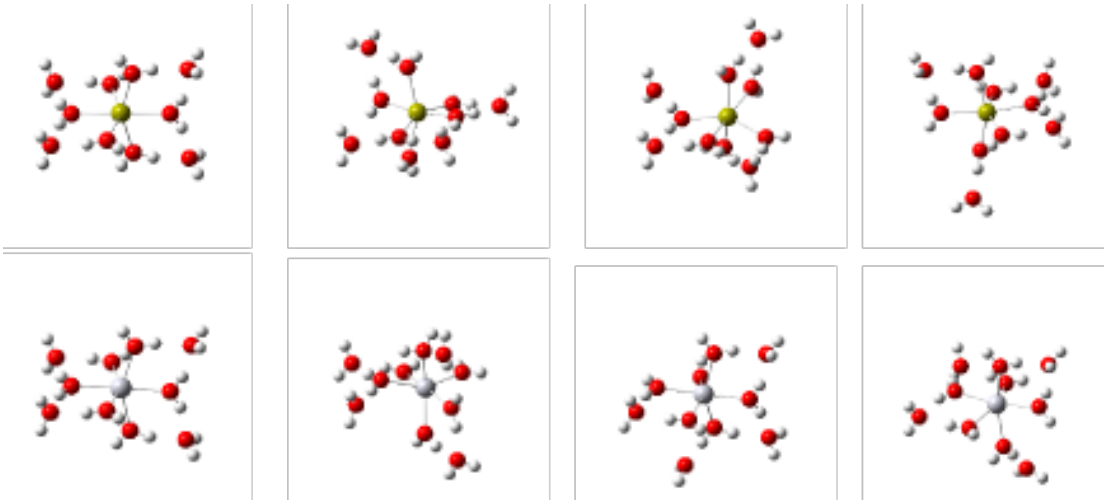

Fig. 4. Structures resulting from the optimization process for decahydrated Ca^{2+} and Hg^{2+} systems where a similar behavior is perceived described in Figure 3. Top: Hydration for Ca^{2+}; lower for Hg^{2+} (B3LYP / LANL2DZ). The links of the first hydration sphere are marked for clarity.

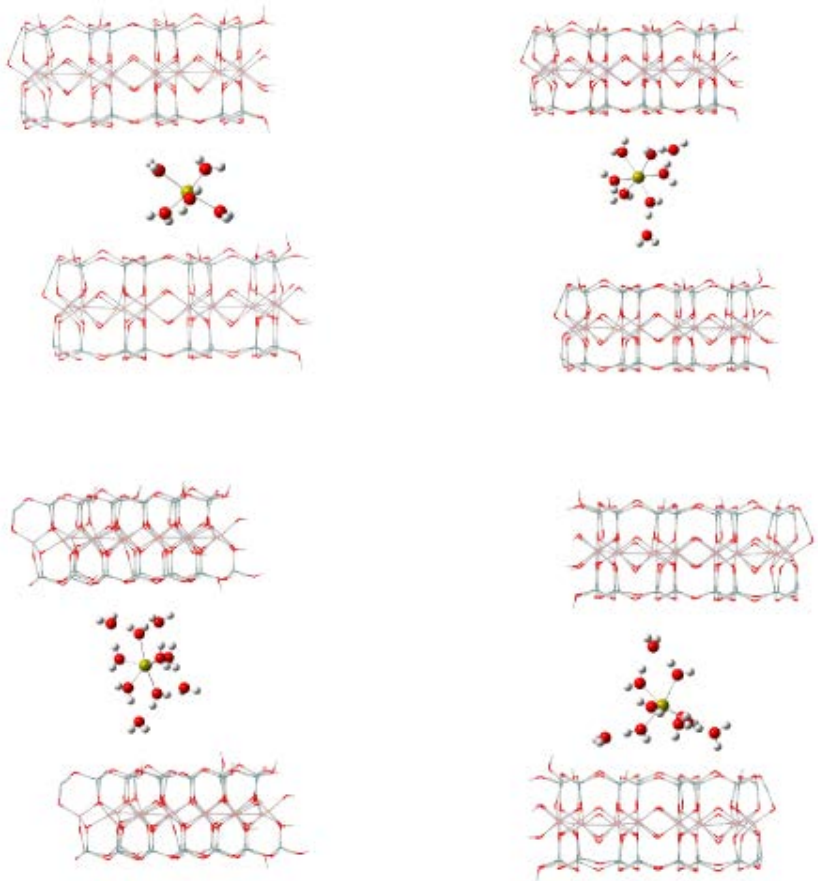

Fig. 5. Illustrative examples of the structures resulting from the modeling of complex-montmorillonite hydrated cation (B3LYP / LANL2DZ: UFF). Top: Resort Ca^{2+} penta (left) and octahydrate (right) with montmorillonite; Bottom: Resort Ca^{2+} decahydrated with montmorillonite.

J. Mex. Chem. Soc. **2018**, *62*(2)
Special Issue

ISSN-e 2594-0317
ISSN 1870-249X

Enthalpies and free energies of reaction.

The usual way of determining the enthalpies of reaction is through the determination of the heats of formation considering the appropriate sums and differences.

$$\Delta_r H°\ (298K) = \Delta_{Productos}\ \Delta_f H°_{Prod}(298K) - \Delta_{Reactivos}\ \Delta_f H°_{React}(298K) \qquad \text{Eq. 5}$$

From equation (5) the enthalpies of reaction for the proposed models can be established from equation (6).

$$Ca^{2+}\cdot H_2O\text{-Montmorillonite} + Hg^{2+}\cdot H_2O \rightleftarrows Hg^{2+}\cdot H_2O\text{-Montmorillonite} + Ca^{2+}\cdot H_2O \quad \text{Eq. 6}$$

where $Ca^{2+}\cdot H_2O$-Montmorillonite and $Hg^{2+}\cdot H_2O$-montmorillonite complexes correspond to the hydrated cation-montmorillonite while $Ca^{2+}\cdot H_2O$ and $Hg^{2+}\cdot H_2O$ represent hydrated cations. A similar process can be applied to determine free energies of reaction. Thus, the respective combinations for both Ca^{2+} and Hg^{2+} were analyzed. As was expected, each of the complexes present several values $\Delta_r H°$ and $\Delta_r G°$ (B3LYP/Lanl2dz:UFF). However, those systems have two coordination spheres between the montmorillonite layers, where the first hydration sphere consists of 6 water molecules and the molecules remaining to a second to give the same signs for $\Delta_r H°$ and $\Delta_r G°$. Specifically, the octahydrate cation-montmorillonite model gave values of ΔrH° = –57.53 kJ / mol and ΔrG °= –60.76 kJ / mol. These values are relatively close to those described experimentally. Thus, this is possible that this complex contributes, preferentially, to Hg^{2+} adsorption on bentonite as suggested in Fig. 6.

It is possible to observe, in Fig. 6, that the Hg^{2+} hydration sphere changes after simulation in solution when it is located between montmorillonite layers. The difference between the experimental values and those obtained by simulation may correspond to the simplification of the proposed models as well as the characteristics of the calculation variables and methods that were used.

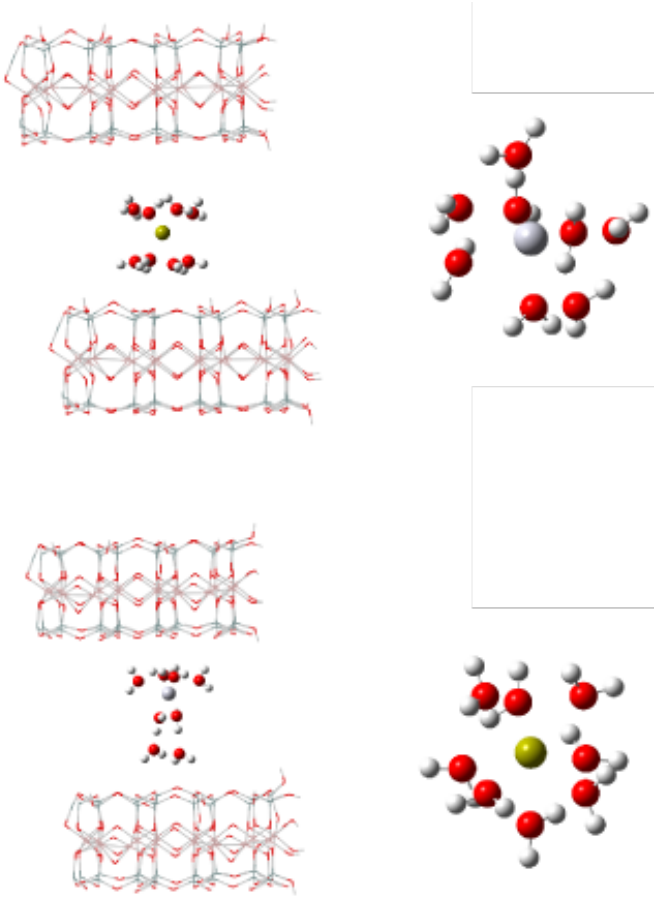

Fig. 6. Preferable combination by $\Delta_r H°$ and $\Delta_r G°$ values of possible complexes involved in the adsorption of Hg^{2+} on bentonite. Top left: Ca^{2+} octahydrate-montmorillonite; top right: Hg^{2+} octahydrate. Lower left: Hg^{2+} octahydrate-montmorillonite complex; bottom left: Ca^{2+} octahydrate.

J. Mex. Chem. Soc. **2018**, *62*(2)
Special Issue

ISSN-e 2594-0317
ISSN 1870-249X

Conclusions

Using both the MINSQ and GAUSSIAN 09 program was possible study the adsorption of Hg (II) from aqueous solution into Ca-bentonite that was also studied experimentally using a batch technique under controlled temperature and constant pressure conditions. Experimental and simulation results correlate the behavior of mercury adsorption on Ca-bentonite because the difference between experimental and simulated values correspond to the simplification of the proposed models as well as to the variables of the calculation methods used using molecular mechanics (UFF) using the DFT method. With the results of the molecular simulation the cation model octahydrate-montmorillonite was established with values of ΔrH ° and ΔrG ° of -57.53 KJ/mol and -60.76 KJ/mol respectively, which are very close to the experimentally described in the adsorption of Hg^{2+} in bentonite.

Acknowledgements

Authors thank Consejo Nacional de Ciencia y Tecnología de los Estados Unidos Mexicanos (CONACyT) for the financial support, and to Richard Lindeke, PhD, Professor Emeritus, University of Minnesota Duluth and U.S. Peace Corps Volunteer, CIATEC, Leon, Mexico, by his English revision to this manuscript. I. Robles is grateful to CONACyT for her Ph.D. scholarship.

References

1. Aylett, B. J. *Polyhedron* **1985**, *4*, 1799-1800.
2. Rodríguez-Sarmiento, D. C.; Pinzón-Bello, J. A. *Appl. Clay Sci.* **2001**, *18*, 173–181.
3. Choi, S.; Jeon, Y.; Kim, E.; Lee, S. *Korean Soc. Environ. Eng.* **1999**, *4*, 81–88.
4. Pavlov, M.; Siegbahn, P. E. M.; Sandstrom, M. *J. Phys. Chem. A* **1998**, *102*, 219.
5. Auerbach, S. M.; Carrado, K. A.; Dutta, P. K. *Handbook of Layered Materials* **2004**, https://books.google.com.mx/books?hl=es&lr=&id=xqTdrzG5DgIC&oi=fnd&pg=PP11&dq=Auerbach,+S.+M.%3B+Carrado,+K.+A.%3B+Dutta,+P.+K.+Handbook+of+Layered+Materials%3B+2004.&ots=TAJV-NOVwG&sig=w62HjoSTgQy4X1f8rafLaeFRChw#v=onepage&q&f=false
6. Soldán, P.; Lee, E. P. F.; Wright, T. G. *J. Phys. Chem. A* **2002**, *106*, 8619–8626.
7. Afaneh, A. T.; Schreckenbach, G.; Wang, F. *J. Phys. Chem. B.* **2014**, *118*, 11271-11283.
8. Afaneh, A. T.; Schreckenbach, G.; Wang, F. *Theor. Chem. Acc.* **2012**, *131*, 1–17.
9. Sawunyama, P.; Bailey, G. W. *J. Phys. Chem. A* **2001**, *105*, 9717–9724.
10. Bush, M. F.; Saykally, R. J.; Williams, E. R. Chem. Phys. Chem. **2007**, *8*, 2245–2253.
11. Chatterjee, A. *J. Chem. Sci.* **2005**, *117*, 533–539.
12. Rappe, A. K.; Casewit, C. J.; Colwell, K. S.; Goddard III, W. A.; Skiff, W. M. *J. Am. Chem. Soc.* **1992**, *114*, 10024–10035.
13. Janeba, D.; Čapková, P.; Weiss, Z. *J. Mol. Model.* **1998**, *4*, 176–182.
14. Janeba, D. *Clay Miner.* **1998**, *33*, 197–204.
15. Becke, A. D. *J. Chem. Phys.* **1993**, *98*, 1372-1380.
16. Wadt, W. R.; Hay, P. J. *J. Chem. Phys.* **1985**, *82*, 284–298.
17. Volke Sepúlveda, T.; Velasco Trejo, J. A.; de la Rosa Pérez, D. A. *Suelos Contaminados por Metales y Metaloides: Muestreo y Alternativas para su Remediación* **2005**, https://books.google.com.mx/books?id=A50ITx37ScsC&printsec=frontcover&dq=Volke+Sep%C3%BAlveda,+T.;+Velasco+Trejo,+J.+A.;+de+la+Rosa+P%C3%A9rez,+D.+A.+Suelos+contaminados+por+metales+y+metaloides:+muestreo+y+alternativas+para+su+remediaci%C3%B3n;+2005.&hl=es&sa=X&ved=0ahUKEwj-jKGK75zbAhUQLKwKHX8_C2kQ6AEILjAB#v=onepage&q&f=false
18. Morel, F. M. M.; Kraepiel, A. M. L.; Amyot, M. *Annual Rev. Ecol. Syst.* **1998**, 29, 543-566.
19. Mason, R. P.; Fitzgerald, W. F.; Morel, F. M. M. *Geochim. Cosmochim. Acta* **1994**, *58*, 3191-3198.
20. Biester, H.; Müller, G.; Schöler, H. F. *Sci. Total Environ.* **2002**, *284*, 191–203.
21. Doula, M.; Ioannou, A.; Dimirkou, A. *Adsorption* **2000**, *6*, 325–335.
22. Skoog, D.; Holler, F.; Nieman, T. *Principios de Análisis Instrumental* **2008**. https://books.google.com.mx/books?id=7FOyZbb7q8UC&dq=Skoog,+D.;+Holler,+F.;+Nieman,+T.

J. Mex. Chem. Soc. **2018**, *62*(2)
Special Issue

ISSN-e 2594-0317
ISSN 1870-249X

+Principios+de+an%C3%A1lisis+instrumental;+2008.&hl=es&sa=X&ved=0ahUKEwifnc2O8JzbAhULYK0KHeQiAIAQ6AEIJzAA
23. Kennedy, J. U.; Murthy, Z. V. P. *Appl. Clay Sci.* **2010**, *50*, 409–413.
24. Kim, E. A.; Masue-Slowey, Y.; Fendorf, S.; Luthy, R. G. *Chemosphere* **2012**, *86*, 648–654.
25. Foo, K. Y.; Hameed, B. H. *Chem. Engin. J.* **2010**, *156*, 2–10.
26. Toor, M.; Jin, B. *Chem. Eng. J.* **2012**, *187*, 79–88.
27. Jeppu, G. P.; Clement, T. P. J. *Contam. Hydrol.* **2012**, 5, 129-170.
28. Dawodu, F. A.; Akpomie, G. K.; Ogbu, I. C. *Int. J. Multidiscip. Sci. Eng.* **2012**, *3*, 9–14.
29. Wankasi, D.; Tarawou, T. J. *Appl. Sci. Environ. Manag.* **2010**, *14*, 1-50.
30. Ho, Y. S.; Porter, J. F.; Mckay, G. *Water, Air, Soil Pollut.* **2002**, *141*, 1–33.
31. Ho, Y. S.; McKay, G. *Process Biochem.* **1999**, *34*, 451–465.
32. Itodo, A. U.; Itodo, H. U. *Life Sci. J.* **2010**, *7*, 31–39.
33. Horsfall Jnr, M.; Spiff, A. I. *Acta Chim. Slov.* **2005**, *52*, 174–181.
34. Robles, I.; Godínez, L. A.; Bustos, E. *ECS Trans.* **2015**, *64*, 13–23.
35. Frisch, M. J.; Trucks, G. W.; Schlegel, H. B.; Scuseria, G. E.; Robb, M. A.; Cheeseman, J. R.; Montgomery, Jr., J. A.; Vreven, T.; Kudin, K. N.; Burant, J. C.; Millam, J. M.; Iyengar, S. S.; Tomasi, J.; Barone, V.; Mennucci, B.; Cossi, M.; Scalmani, G.; P, J. A. *Gaussian 03*, Revision E.01 **2004**. http:/ http://gaussian.com/g03citation/
36. Ulman, A. *An Introduction to Ultrathin Organic Films Academic*. Academic Press, **1991**. https://www.elsevier.com/books/an-introduction-to-ultrathin-organic-films/ulman/978-0-08-092631-5
37. Olsson, S.; Karnland, O. Characterisation of Bentonites from Kutch, India and Milos, Greece - some Candidate Tunnel Back-Fill Materials? Stockholm, **2009**. http://www.iaea.org/inis/collection/NCLCollectionStore/_Public/41/038/41038317.pdf
38. Mignon, P.; Ugliengo, P.; Sodupe, M.; Hernandez, E. R. *Phys. Chem. Chem. Phys.* **2010**, *12*, 688–697.
39. Viani, A.; Gualtieri, A. F.; Artioli, G. *Am. Mineral.* **2002**, *87*, 966–975.
40. Kohagen, M.; Mason, P. E.; Jungwirth, P. *J. Phys. Chem. B* **2014**, *118*, 7902–7909.
41. Jalilehvand, F.; Spangberg, D.; Lindqvist-Reis, P.; Hermansson, K.; Persson, I.; Sandstrom, M. *J. Am. Chem. Soc.* **2001**, *123*, 431–441.
42. Megyes, T.; Grósz, T.; Radnai, T.; Bakó, I.; Pálinkás, G. *J. Phys. Chem. A* **2004**, *108*, 7261–7271.
43. Bakó, I.; Hutter, J.; Pálinkás, G. *J. Chem. Phys.* **2002**, *117*, 9838–9843.
44. Badyal, Y. S.; Barnes, A. C.; Cuello, G. J.; Simonson, J. M. *J. Phys. Chem. A* **2004**, *108*, 11819– 11827.
45. D'Angelo, P.; Petit, P. E.; Pavel, N. V. *J. Phys. Chem. B* **2004**, *108*, 11857–11865.
46. Zavitsas, A. A. *J. Phys. Chem. B* **2005**, *109*, 20636–20640.
47. Sobolev, O.; Cuello, G. J.; Román-Ross, G.; Skipper, N. T.; Charlet, L. *J. Phys. Chem. A* **2007**, *111*, 5123–5125.
48. D'Angelo, P.; Migliorati, V.; Mancini, G.; Barone, V.; Chillemi, G. *J. Chem. Phys.* **2008**, *128*, 84502-84508.
49. Mancini, G.; Sanna, N.; Barone, V.; Migliorati, V.; D'Angelo, P.; Chillemi, G. *J. Phys. Chem. B* **2008**, *112*, 4694–4702.
50. Johansson, J. *Acta Chem. Scand.* **1971**, *25*, 2787–2798.
51. Maliarik, M.; Persson, I. *Magn. Reson. Chem.* **2005**, *43*, 835–842.
52. Babu, C. S.; Lim, C. *J. Phys. Chem. A* **2006**, *110*, 691–699.
53. Chillemi, G.; Mancini, G.; Sanna, N.; Barone, V.; Della Longa, S.; Benfatto, M.; Pavel, N. V.; D'Angelo, P. *J. Am. Chem. Soc.* **2007**, *129*, 5430–5436.
54. Riccardi, D.; Guo, H. B.; Parks, J. M.; Gu, B.; Liang, L.; Smith, J. C. *J. Chem. Theory Comput.* **2013**, *9*, 555–569.
55. Berghout, A.; Tunega, D.; Zaoui, A. *Clays Clay Miner.* **2010**, *58*, 174–187.
56. Al-Saidi, W. a.; Voora, V. K.; Jordan, K. D. *J. Chem. Theory Comput.* **2012**, *8*, 1503–1513.
57. Scholtzová, E.; Tunega, D.; Madejová, J.; Pálková, H.; Komadel, P. *Vib. Spectrosc.* **2013**, *66*, 123– 131.
58. Tunega, D.; Haberhauer, G.; Gerzabek, M. H.; Lischka, H. *Langmuir* **2002**, *18*, 139–147.
59. Ochterski, J. W.; Ph, D. Thermochemistry in Gaussian, **2013**. http://organ.chem.elte.hu/farkas/teach/thermo.pdf, accessed in January 2013.